

place which is only detectable in compounds of very low Debye temperatures.

From these results, conclusions can be drawn to explain qualitatively the observed effects of  $\text{Co}^{57}$  in cobaltous compounds.<sup>4,5</sup> In the perfectly stoichiometric compounds of  $\text{Co}^{57}$  in  $\text{CoCl}_2$ ,  $\text{CoSO}_4$ , and  $(\text{NH}_4)_2\text{Fe}(\text{SO}_4)_2$ , all of which have low Debye temperatures, ferrous and ferric ions are observed simultaneously.<sup>5</sup> In  $\text{CoO}$  doped with  $\text{Co}^{57}$ , which has a high Debye temperature, only  $\text{Fe}^{2+}$  is observed if the lattice is of perfect stoichiometry.<sup>36</sup> On the other hand, in  $\text{CoO}$  and  $\text{NiO}$  samples, which contain cation vacancies, both  $\text{Fe}^{2+}$  and  $\text{Fe}^{3+}$  charge states are detected.<sup>5</sup>

This seems to indicate that the distortion through the  $\text{Co}^{57}$   $K$  capture and subsequent processes is not large enough to destroy the relative strong bonding (high  $\Theta_D$ ) of perfect compounds, and that higher valence states can only be stabilized if vacancies are present. On the

other hand,  $\text{Fe}^{3+}$  charge states can be established in compounds of perfect lattice structure (no vacancies) which have low  $\Theta_D$ . There the original bonding is decoupled and new types of bonding can be established. This interpretation is consistent with the experimental results and is able to solve most of the controversy concerning the origin of charge states in various compounds containing  $\text{Co}^{57}$ .

Measurements are in progress using  $\text{Te}^{125m}$  in  $\text{Na}_2\text{TeO}_3$ ,  $\text{TeO}_3$ ,  $\text{Na}_2\text{TeO}_4$ , and other tellurium compounds in order to obtain further information about the processes involved.

#### ACKNOWLEDGMENTS

We wish to thank Professor Rudolf L. Mössbauer for his interest in this investigation and Dr. Dietrich Schroer for many helpful discussions about the problems of this work. We are also pleased to acknowledge the support of the Bundesministerium für Wissenschaftliche Forschung, Bonn, Germany.

<sup>36</sup> H. N. Ok and J. G. Mullen, *Phys. Rev.* **168**, 550 (1968).

### Effective Density of Phonon States for $\text{NdCl}_3$ from Vibronic Spectra and Applications to Ion-Lattice Interactions\*

E. COHEN,† L. A. RISEBERG,† AND H. W. MOOS‡

*Department of Physics, The Johns Hopkins University, Baltimore, Maryland 21218*

(Received 13 July 1967; revised manuscript received 20 June 1968)

An effective density of phonon states of  $\text{NdCl}_3$  has been extracted from the vibronic spectra accompanying several electronic transitions of  $\text{Pr}^{3+}$  and  $\text{Nd}^{3+}$ . The derived  $g^*(\omega)$  has a very similar structure for all parent electronic transitions. Anomalies in the vibronic spectra occur for certain optical phonons, and are ascribed to interactions of pairs of  $\text{Nd}^{3+}$  ions via the phonon field. Use is made of the derived  $g^*(\omega)$  in explaining various features of phonon-induced relaxation.

#### I. INTRODUCTION

CERTAIN phenomena arising from the interaction of paramagnetic ions with lattice vibrations are strongly dependent on the structure of the phonon frequency distribution function  $g(\omega)$  of the particular host crystal. Examples are line broadening, multiphonon relaxation, and vibronic transitions. Therefore, it is essential to know the structure of  $g(\omega)$ . Common insulating rare-earth crystals have not been generally studied by inelastic neutron scattering. However, the vibronic spectra accompanying rare-earth electronic transitions provide important information regarding the density of phonon states, since the structure of the

vibronics is related to the structure of  $g(\omega)$ .<sup>1-4</sup> In this study, we have extracted an effective density of phonon states  $g^*(\omega)$  from several transitions of  $\text{Nd}^{3+}$  and  $\text{Pr}^{3+}$  in  $\text{NdCl}_3$ . Although this  $g^*(\omega)$  is not intended to replace the detailed density of phonon states, it is nevertheless valuable, because it manifests those features of the true  $g(\omega)$  which enter into ion-lattice interaction phenomena.

Although the approximations assumed are in most cases valid, there are irregularities for several particular vibronic transitions of  $\text{Nd}^{3+}$  involving optical phonons. The energies of the phonons involved are precisely

<sup>1</sup> W. M. Yen, W. C. Scott, and A. L. Schawlow, *Phys. Rev.* **136**, A271 (1964).

<sup>2</sup> M. V. Hobden, *Phys. Letters* **15**, 10 (1965).

<sup>3</sup> E. Cohen and H. W. Moos, *Phys. Rev.* **161**, 258 (1967); **161**, 268 (1967).

<sup>4</sup> G. F. Imbusch, dissertation, Stanford University, 1964 (unpublished).

\* Supported by NASA under Grant No. NsG 361.

† Present address: Bell Telephone Laboratories, Murray Hill, N.J. 07971.

‡ Alfred P. Sloan Foundation Fellow.

equal to the energies of excited Stark components of the ground multiplet ( $^4I_{9/2}$ ). Such a resonance is manifested in an unusual discrepancy in the vibronic intensity in one case and in an anomalous Zeeman effect in another.

The derived  $g^*(\omega)$  has been applied in the examination of phonon-induced relation. Various features of line broadening have been explained in terms of the relative densities of phonon modes. The extreme broadness of certain higher-lying Stark levels is ascribed to the presence of lower Stark levels for which the energy separation corresponds to a region of high  $g^*(\omega)$ .

## II. PHONON FREQUENCY DISTRIBUTION FUNCTION FROM VIBRONIC SPECTRA

It has been shown previously that the electric-dipole transition probability for vibronic transitions is given by the approximate expression<sup>3</sup>

$$W = (2\pi/\hbar) |\langle \chi_A^{(0)} | P^{[1]} | \chi_B^{(1)} \rangle|^2 g(\omega), \quad (1)$$

where  $g(\omega)$  is the density of phonon modes,<sup>5</sup>  $\chi$  is the product of the phonon state function and the electronic state function  $\psi$ , the electronic transitions are assumed to be infinitely narrow, and<sup>3</sup>

$$\begin{aligned} \langle \chi_A^{(0)} | P^{[1]} | \chi_B^{(1)} \rangle = & \langle \psi_a | P^{[1]} | \psi_b \rangle \left( \frac{\hbar}{2\omega_{k\Gamma}} \right)^{1/2} \left( \frac{\langle \psi_a | f_{k\Gamma^s} | \psi_a \rangle}{-\hbar\omega_{k\Gamma}} + \frac{\langle \psi_b | f_{k\Gamma^s} | \psi_b \rangle}{\hbar\omega_{k\Gamma}} \right) \\ & + \sum_{p \neq a, b} \left( \frac{\hbar}{2\omega_{k\Gamma}} \right)^{1/2} \left\{ \frac{\langle \psi_a | f_{k\Gamma^s} | \psi_p \rangle \langle \psi_p | P^{[1]} | \psi_b \rangle}{E_a - (E_p + \hbar\omega_{k\Gamma})} + \frac{\langle \psi_a | P^{[1]} | \psi_p \rangle \langle \psi_p | f_{k\Gamma^s} | \psi_b \rangle}{(E_b + \hbar\omega_{k\Gamma}) - E_p} \right\}. \quad (2) \end{aligned}$$

It is observed for transitions of  $\text{Pr}^{3+}$  and  $\text{Nd}^{3+}$  in rare-earth chlorides that the polarization and strength of the vibronics reflects, to a large extent, the polarization and strength of the parent transition.<sup>6</sup> This indicates that in Eq. (2) it is the first term that makes the most significant contribution to the vibronic spectrum; the intermediate states are products of phonon states and only the initial and final electronic states. Since only  $4f^n$  crystalline wave functions are involved, it is likely that the matrix elements of Eq. (2) are not very dependent on the particular features of the lattice distortion for a given phonon. This is reasonable because  $4f$  crystalline wave functions are relatively confined in space and more spherical compared with the  $5d$  wave functions. In addition, a large part of the vibronic spectrum consists of broad, unpolarized bands, on which are superimposed sharp, polarized peaks. The main contribution to  $g(\omega)$  is thus due to these broad bands. Since these bands arise from the sum of many phonon modes of low symmetry having the same  $\omega$  (rare-earth chlorides have 24 branches at a general point of the Brillouin zone), individual variations in  $\langle \psi_p | f_{k\Gamma^s} | \psi_p \rangle$  for a given  $\psi_p$  are averaged out. Also, the dependence of the matrix elements on the electronic states involved ( $\psi_a, \psi_b$ ) is probably not very critical, as can be seen from the observed data. Any variation that is observed is generally in the relative strength of the sharp peaks. It should be noted that in the case of  $\text{MgO}:\text{V}^{2+}$  the vibronic transitions observed by Imbusch<sup>4</sup> reflect almost identically the density of phonon

states as determined by Peckham.<sup>7</sup> Furthermore, Timusk and Buchanan<sup>8</sup> have obtained excellent experimental agreement with neutron diffraction data for the vibronic sidebands of  $\text{KBr}:\text{Sm}^{2+}$ .

In view of these approximations, the transition probability for vibronic absorption is written

$$W = |\langle \psi_a | P^{[1]} | \psi_b \rangle|^2 C [g^*(\omega)/\omega^3], \quad (3)$$

where the factor  $C$  contains the ion-lattice interaction matrix elements.

It is thus possible to extract  $g^*(\omega)$  from the vibronic spectra associated with sharp, isolated electronic transitions. The level involved must contain only a single Stark component because of the impossibility of extracting this information from the superimposed vibronics of several Stark components.

This procedure was applied to the vibronic absorption transitions associated with the  $^3H_4(\mu = \pm 2)$  to  $^3P_0(\mu = 0)$  of  $\text{Pr}^{3+}$  and the  $^4I_{9/2}(\mu = \pm \frac{5}{2})$  to  $^2P_{1/2}(\mu = \pm \frac{1}{2})$  of  $\text{Nd}^{3+}$ , both in  $\text{NdCl}_3$ . Polarized absorption spectra were obtained photoelectrically under high resolution at 1.5°K. Using (3), the effective phonon distribution functions  $g^*(\omega)$  have been extracted from these spectra and are shown in Figs. 1-3.

The peaks correspond to phonon branches whose symmetry properties have been determined by other means.<sup>3</sup> It has also been demonstrated that these vibronics are in fact due only to single phonon excitations.<sup>3</sup> It should be pointed out that the interaction  $f_{k\Gamma^s}$  depends linearly on  $\omega$  for acoustical phonons,<sup>9</sup> and

<sup>5</sup> J. C. Phillips, Phys. Rev. **104**, 1263 (1956).

<sup>6</sup> The most striking example of this is the transition  $^3H_4(\mu = \pm 2)$  to  $^3P_0(\mu = 0)$  of  $\text{Pr}^{3+}$  in  $\text{NdCl}_3$ , for which the parent transition is  $\sigma$ -polarized and the vibronics are  $\sigma$ -polarized as well (Ref. 3).

<sup>7</sup> G. Peckham, Proc. Phys. Soc. (London) **90**, 657 (1967).

<sup>8</sup> T. Timusk and M. Buchanan, Phys. Rev. **164**, 345 (1967).

<sup>9</sup> E. Cohen, dissertation, The Johns Hopkins University, 1967 (unpublished).

thus the vibronic intensity has an additional factor of  $\omega^2$  relative to the case of optical phonons. However, this should be included to maintain a consistent interpretation of our  $g^*(\omega)$  as an effective density of phonon states reflecting the strength of the ion-lattice interaction.

A notable feature of Figs. 1-3 is the relative importance of the optical phonon region as compared with the acoustical region. This is not unreasonable in view of the fact that 21 of the total of 24 phonon branches are optical modes. If one assumes a cutoff of acoustical phonons at about  $100 \text{ cm}^{-1}$ , then the area under the optical phonon region is approximately 40 times greater than the area under the acoustical phonons.

Comparing the figures, one sees that, except in the cases of a few sharp peaks (due to phonons having high symmetries), the derived  $g^*(\omega)$  are very similar in all three cases. The unpolarized broad bands are repeated. The positions of the high symmetry peaks are un-

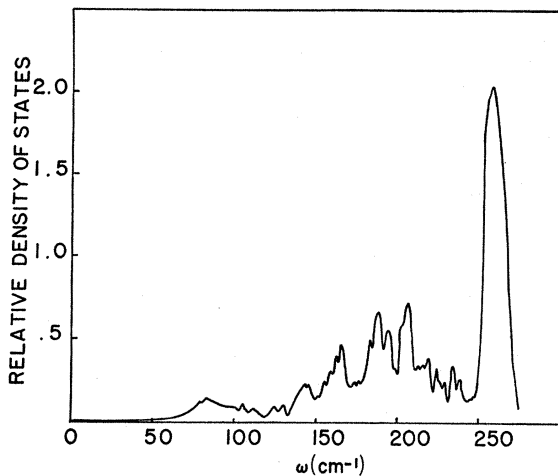


FIG. 1. Phonon frequency distribution function from  $\sigma$ -polarized vibronics accompanying  ${}^3H_4(\mu=\pm 2) \rightarrow {}^3P_0(\mu=0)$  transition of  $\text{Pr}^{3+}$  in  $\text{NdCl}_3$  at  $1.5^\circ\text{K}$  ( $\sigma$  polarization is allowed,  $\pi$  vibronics are weak.)

changed and their relative heights are only somewhat altered due to the residual dependence of the matrix elements on the electronic transitions. The only large variation is observed for the phonons around  $80 \text{ cm}^{-1}$  (which appear enhanced in the vibronics of  ${}^3P_0$  or  $\text{Pr}^{3+}$  in all rare-earth chlorides). The large variation in the vibronic intensity for the  $260\text{-cm}^{-1}$  phonon in the  $\text{Nd}^{3+}$  spectra represents a special case which is treated in the next section.

### III. ANOMALIES IN THE VIBRONIC SPECTRA OF $\text{Nd}^{3+}$

Several anomalous effects have been observed for specific optical phonons. They are manifested by a discrepancy in the vibronic intensity or by an anomalous Zeeman effect for the particular vibronic transitions.

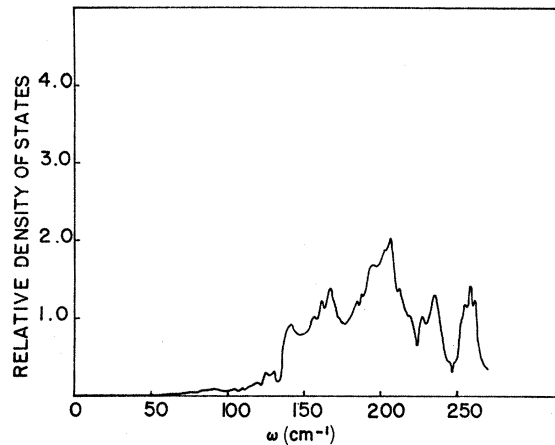


FIG. 2. Phonon frequency distribution function from vibronics accompanying  ${}^4I_{9/2}(\mu=\pm \frac{5}{2}) \rightarrow {}^2P_{1/2}(\mu=\pm \frac{1}{2})$   $\sigma$ -polarized transition of  $\text{Nd}^{3+}$  in  $\text{NdCl}_3$  at  $1.5^\circ\text{K}$ .

Although they are not useful from the point of view of extracting  $g^*(\omega)$ , they are nevertheless interesting in their own right.

Figure 4 shows the energy of two vibronic transitions associated with the electronic transition  ${}^4I_{9/2}(\mu=\pm \frac{5}{2}) \rightarrow {}^2P_{1/2}(\mu=\pm \frac{1}{2})$  as a function of applied magnetic field parallel to the  $c$  axis, at  $1.4^\circ\text{K}$ . At this temperature, for magnetic fields larger than  $10 \text{ kOe}$ , absorption takes place only from the lower Zeeman component of the ground state. The resulting Zeeman effect of most vibronic transitions associated with the above-mentioned electronic transition is a simple two-line pattern with slopes of 1.8 and 2.6 Lorentz units. The Zeeman pattern of the vibronics involving phonons of energy  $124$  and  $129 \text{ cm}^{-1}$ , shown in Fig. 4, is not at all like the normal case. Both vibronics show a large number of polarized Zeeman components which are closely spaced. The solid lines in Fig. 4 correspond to strong absorption

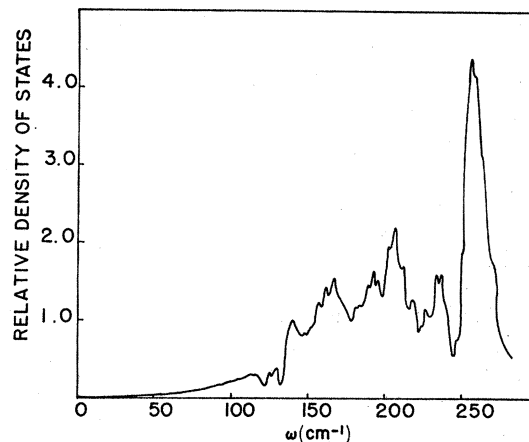


FIG. 3. Phonon frequency distribution function from vibronics accompanying  ${}^4I_{9/2}(\mu=\pm \frac{5}{2}) \rightarrow {}^2P_{1/2}(\mu=\pm \frac{1}{2})$   $\pi$ -polarized transition of  $\text{Nd}^{3+}$  in  $\text{NdCl}_3$  at  $1.5^\circ\text{K}$ .

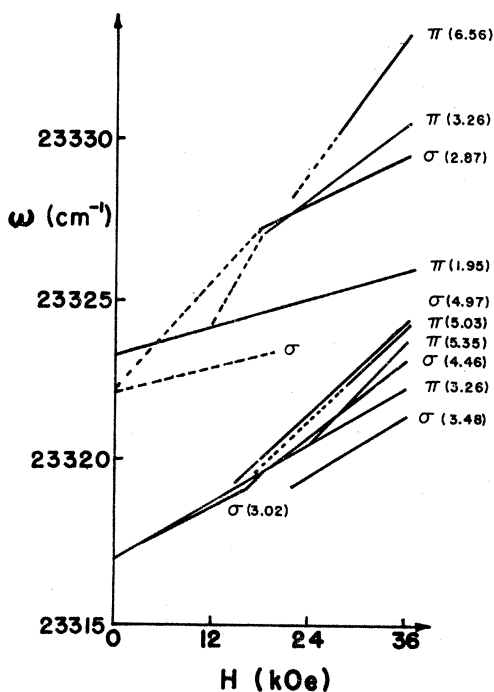


FIG. 4. Anomalous Zeeman effect of vibronic transitions accompanying the electronic transition  ${}^4I_{9/2}(\mu = \pm\frac{5}{2}) \rightarrow {}^2P_{1/2}(\mu = \pm\frac{1}{2})$  of  $\text{Nd}^{3+}$  in  $\text{NdCl}_3$  at  $23\,193.2\text{ cm}^{-1}$ . The solid lines correspond to strong transitions for which the slopes are given (in Lorentz units). The dashed lines correspond to weak lines whose energy could be determined for two field values only. Observation was done at  $1.4^\circ\text{K}$ .

transitions whose energy has been determined for a large number of magnetic-field values. The dashed lines represent weak absorption transitions, and for these the energy could be determined for two field values only. The deviation of the slopes of all of the observed Zeeman components from those of a normal vibronic transition is striking. For temperatures slightly higher than  $1.5^\circ\text{K}$ , the  $\pi$  components with slopes of 5.35 and 5.03 Lorentz units and the  $\sigma$  components with slopes of 4.46 and 4.97, of the lower energy vibronics, are unresolved. However, the large slopes (5.3 in  $\pi$  and 4.5 in  $\sigma$ ) are independent of temperature (up to  $77^\circ\text{K}$ ).

The appearance of a large number of Zeeman components suggests the presence of an interaction between the  $\text{Nd}^{3+}$  ion and its neighboring  $\text{Nd}$  ions. It is observed that the phonons involved have energies which match those of the first two excited Stark components of the ground multiplet;  ${}^4I_{9/2}(\mu = \pm\frac{1}{2})$  lies at  $123.7\text{ cm}^{-1}$  and  ${}^4I_{9/2}(\mu = \pm\frac{3}{2})$  at  $129.6\text{ cm}^{-1}$ . This means that a resonance interaction between the ions takes place via the phonon field. The discontinuities in the slopes of the energies of the vibronic Zeeman components versus magnetic field are therefore probably due to the perfect matching of the ionic system energies with those of the phonons. Assuming an interaction between a pair of  $\text{Nd}^{3+}$  ions via the phonon field in the presence of a magnetic field ( $H = V_{12} + V_{eV} + H_M$ ), the following degenerate

states interact:  $|\psi_{1g}\rangle|\psi_{2g}\rangle|Q1\rangle$ ,  $|\psi_{1g}\rangle|\psi_{2e}\rangle|Q0\rangle$ ,  $|\psi_{1e}\rangle|\psi_{2g}\rangle|Q0\rangle$ . Here 1 and 2 designate the two interacting ions;  $g$  and  $e$  the ionic ground and excited states, respectively; and  $|Q0\rangle$  and  $|Q1\rangle$  the phonon ground and excited states, respectively. Using these states and the known splitting factors for  ${}^4I_{9/2}(\mu = \pm\frac{1}{2}, \pm\frac{3}{2})$ , the splitting factors obtained for the initial vibronic states are too small to account for the large observed slopes.

The other case of an observed anomaly is for the phonon with energy  $259\text{ cm}^{-1}$ , which is exceptionally strong, as is seen in Fig. 1. This vibronic appears strongly in all trichlorides. In the case of  $\text{Nd}^{3+}$ , as is shown in Figs. 2 and 3, the ratio of the intensities for the two polarizations is unusually high, in view of the fact that both polarizations are allowed for a phonon of this symmetry. One significant feature is that the upper two Stark components of the  $\text{Nd}^{3+}$  ground multiplet (at  $260$  and  $261\text{ cm}^{-1}$ ) fall within the width of the observed vibronic transition. Simple ion-pair absorption is excluded, because with their intensities equal to at most  $10^{-5}$  of a single-ion transition,<sup>10</sup> they are two orders of magnitude weaker than vibronics, whose intensities are generally about  $10^{-3}$  of the parent transition.<sup>11</sup>

#### IV. APPLICATION TO ORBIT-LATTICE RELAXATION PROCESSES

The derived  $g^*(\omega)$  can be utilized in a semiquantitative way to determine the probable nature of phonon-induced relaxation processes.<sup>1,12</sup> For example, certain features of the phonon broadening of the components of a rare-earth Stark multiplet can be explained by reference to  $g^*(\omega)$ .

The transition rate for a single phonon decay process between states  $p$  and  $q$  is given by the following expression:

$$W = (\pi/\omega_{k\Gamma}) |\langle \psi_p | f_{k\Gamma^s} | \psi_q \rangle|^2 (n_{k\Gamma} + 1) g(\omega), \quad (4)$$

where  $n_{k\Gamma}$  is the occupation number of the phonon mode corresponding to  $k$ ,  $\Gamma$ , and  $s$ , and  $f_{k\Gamma^s}$  is the same

TABLE I. Stark levels of  $W({}^4I_{15/2})$  of  $\text{Nd}^{3+}$  in  $\text{NdCl}_3$ : Information has been taken from Ref. 15. Approximate linewidths taken from absorption spectra in Ref. 15 for 50%  $\text{Nd}^{3+}$  in  $\text{LaCl}_3$ .

Designation	Energy	$\pm\mu$	Representation in $C_{3h}$	Approximate linewidth (cm <sup>-1</sup> )
$W_1$	0.0	Relative intensities are 1:1:1:1:1:1	$\Gamma_7, \Gamma_8$	<2
$W_2$	73.1		$\Gamma_7, \Gamma_8$	<2
$W_3$	122.9		$\Gamma_{11}, \Gamma_{12}$	8
$W_5$	210.2		$\Gamma_7, \Gamma_8$	18
$W_6$	284.9		$\Gamma_{11}, \Gamma_{12}$	20

<sup>10</sup> E. S. Dorman, dissertation, The Johns Hopkins University, 1965 (unpublished).

<sup>11</sup> W. D. Partlow (private communication).

<sup>12</sup> A. Kiel, Phys. Rev. **126**, 1292 (1962).

dynamic crystalline field atomic operator appearing in Eq. (2). Although the matrix elements involved in Eq. (4) are different from those of Eq. (2), it is not an unreasonable assumption that the spontaneous phonon transition rate is approximately proportional to the effective density of states  $g^*(\omega)$  obtained in Sec. II above, consistent with any selection rules on the  $\langle \psi_p | f_{kr}^s | \psi_q \rangle$ . Since there are strong low-symmetry bands underlying the higher symmetry peaks, selection rules will be of secondary importance, relative to  $g^*(\omega)$ . Such an approximation is useful for our discussion of intramultiplet phonon decay.

One common observation is the much larger broadenings for the higher levels in a rare-earth Stark multiplet.<sup>13,14</sup> For rare-earth trichlorides, typical separations between adjacent Stark levels are less than 100 cm<sup>-1</sup>. The strongest peaks in  $g^*(\omega)$  fall in the phonon energy region of 130–260 cm<sup>-1</sup>; therefore, it is likely that optical phonon crossover relaxation from high-lying Stark levels to those around 200 cm<sup>-1</sup> lower dominates the decay, rather than transitions via low-energy phonons to the Stark component immediately below. The lower-lying Stark levels are much narrower, because for splittings up to 100 cm<sup>-1</sup> relaxation must necessarily involve the low-energy phonon region, for which  $g^*(\omega)$  is relatively much lower.

For example, the  $W(^4I_{15/2})$  multiplet of Nd<sup>3+</sup> in LaCl<sub>3</sub> has been studied in absorption by Varsanyi and Dieke.<sup>15</sup> Details of the multiplet are given in Table I. Although the absorption has been done for high concentrations of Nd<sup>3+</sup> (5%, 50%) in LaCl<sub>3</sub>, the situation is the same as 100% NdCl<sub>3</sub>, except for small shifts in the phonon energies and in the parent electronic transition.

The striking feature of this multiplet is the extreme breadth of the  $W_5$  and  $W_6$  levels. But these levels are the only two for which there are separations to lower Stark levels which fall in the region of high  $g^*(\omega)$ . Although the relaxation is probably due in large part to the underlying low-symmetry bands, one can also consider the resonances that exist between the energy separations and the higher symmetry peaks in  $g^*(\omega)$ .

The separation of  $W_5$  from  $W_2$  is 137.1 cm<sup>-1</sup>. There is a peak in  $g^*(\omega)$  corresponding to a mode at 139 cm<sup>-1</sup>, transforming as  $T_1+K_1$  or  $T_1+\Gamma_4^-$  of  $C_{6h}^2$ . (These are equivalent in terms of vibronic selection rules.) In

LaCl<sub>3</sub>, this mode is shifted to 138 cm<sup>-1</sup>. Figures 1–3 show how strong the model is. The symmetry of this mode reduces<sup>16</sup> to  $\Gamma_1+\Gamma_2+\Gamma_3$  of  $C_{3h}$ , and the product  $(\Gamma_7, \Gamma_8) \times (\Gamma_1+\Gamma_2+\Gamma_3) \times (\Gamma_7, \Gamma_8)$  contains  $\Gamma_1$  and therefore the  $W_5 \rightarrow W_2$  transition is allowed. In almost all cases it is found that reduction to the site symmetry includes sufficient representations to permit a transition. Now  $W_5 \rightarrow W_1$  is also a possibility, since the NdCl<sub>3</sub> mode at 217 cm<sup>-1</sup> (210 cm<sup>-1</sup> in LaCl<sub>3</sub>) is nearly resonant.

The  $W_6 \rightarrow W_3$  transition at 162 cm<sup>-1</sup> falls in a region with large  $g^*(\omega)$ . There is a near resonance with several strong peaks, and the mode assignments are consistent with an allowed transition. Under the assumption that the coupling constant is nearly equal for all modes, the broadening, as seen from Eq. (4), is proportional to  $g^*(\omega)/\omega$ . The ratio of the  $W_5$  and  $W_6$  linewidths is observed to be consistent with this dependence, i.e.,

$$\frac{\Delta\omega(W_5)}{\Delta\omega(W_6)} \approx \frac{162 g^*(137 \text{ cm}^{-1})}{137 g^*(162 \text{ cm}^{-1})}. \quad (5)$$

Additional evidence of this type can be seen by comparing the  $W_5$  and  $W_6$  linewidths with the slit-limited cases of  $W_2$  and  $W_1$ . The ratios of the linewidths are at least 10. This is consistent with the relative values of  $g^*(\omega)/\omega$  as obtained from Figs. 1–3.

This multiplet is a particular example, but the behavior is consistent throughout the energy levels of the rare earths. Another striking case is the  $W(^6H_{9/2}, ^6F_{11/2})$  multiplet of Dy<sup>3+</sup> in LaCl<sub>3</sub>, studied in absorption by Varsanyi and Dieke.<sup>17</sup> The first ten Stark levels are spaced over 106 cm<sup>-1</sup>, and none of these is broadened more than 8 cm<sup>-1</sup>. The highest Stark level lies 173 cm<sup>-1</sup> above the lowest and is about 15 cm<sup>-1</sup> broad.

In addition to the case of single-phonon decay, as manifested in linewidths, the structure of  $g^*(\omega)$  governs multiphonon decay as manifested in fluorescence quenching. Systematic studies of multiphonon relaxation and its temperature dependence in LaCl<sub>3</sub> have indicated that such decay is due to the emission of phonons in the high-energy optical region.<sup>18,19</sup> This is a consequence of the fact that these processes correspond to the lowest orders possible as well as the fact that the phonons involved have the highest densities.

<sup>16</sup> G. F. Koster, in *Space Groups and the Representations* (Academic Press Inc., New York, 1957).

<sup>17</sup> F. Varsanyi and G. H. Dieke, J. Chem. Phys. **36**, 835 (1962).

<sup>18</sup> W. D. Partlow and H. W. Moos, Phys. Rev. **157**, 252 (1967).

<sup>19</sup> L. A. Riseberg, W. B. Gandrud, and H. W. Moos, Phys. Rev. **159**, 262 (1967).

<sup>13</sup> F. Varsanyi and G. H. Dieke, J. Chem. Phys. **31**, 1066 (1959).

<sup>14</sup> S. Yatsiv, Physica **28**, 521 (1962).

<sup>15</sup> F. Varsanyi and G. H. Dieke, J. Chem. Phys. **33**, 1616 (1960).